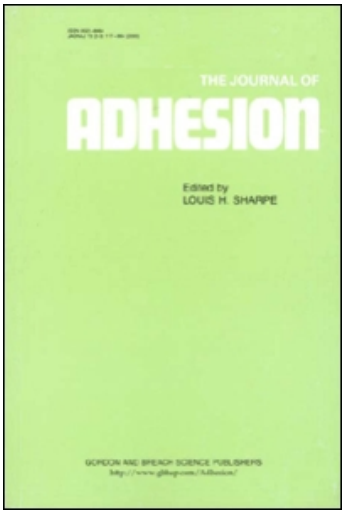

The Journal of Adhesion
Publication details, including instructions for authors and subscription information:
http://www.informaworld.com/smpp/title~content=t713453635

Nanocomposites of Epoxy with Electrospun Carbon Nanofibers: Mechanical Behavior

Erol Sancaktar[a]; Darunee Aussawasathien[b]
[a] Polymer Engineering Department, University of Akron, Akron, OH, U.S.A. [b] National Metal and Materials Tech. Center, Pathumthani, Thailand

To cite this Article Sancaktar, Erol and Aussawasathien, Darunee(2009) 'Nanocomposites of Epoxy with Electrospun Carbon Nanofibers: Mechanical Behavior', The Journal of Adhesion, 85: 4, 160 — 179
To link to this Article: DOI: 10.1080/00218460902881758
URL: http://dx.doi.org/10.1080/00218460902881758

The Journal of Adhesion, 85:160–179, 2009

ISSN: 0021-8464 print/1545-5823 online
DOI: 10.1080/00218460902881758

Taylor & Francis
Taylor & Francis Group

Nanocomposites of Epoxy with Electrospun Carbon Nanofibers: Mechanical Behavior

Erol Sancaktar[1] and Darunee Aussawasathien[2]
[1]Polymer Engineering Department, University of Akron, Akron, OH, U.S.A.
[2]National Metal and Materials Tech. Center, Pathumthani, Thailand

Electrospun polyacrylonitrile (PAN) fiber precursor-based carbon nanofiber (CNF) mats were produced and impregnated with epoxy resin. The mechanical properties of as-prepared nanofibers in the mat and short fiber filled epoxy nanocomposite forms were determined to demonstrate the effect of fiber aspect ratio on those properties. The experimental results reveal that epoxy nanocomposites containing electrospun carbon nanofibers (ECNF) with high fiber aspect ratio in the non-woven mat form yield better mechanical properties than those filled with short ECNFs. The ECNF mat in epoxy nanocomposites provides better homogeneity and easier preparation than short ECNFs. Mechanical properties of ECNF mat-epoxy nanocomposites, which were obtained using tensile and flexural tests, such as stiffness, increased, while toughness and flexural strength decreased, compared with the neat epoxy resin. Dynamic mechanical analysis results showed higher modulus for ECNF mat-epoxy nanocomposites, compared with those for neat epoxy resin and short ECNF-epoxy nanocomposites. The ECNF-epoxy nanocomposites had higher storage and Young's moduli with 1.23, 3.56 and 9.28 wt% ECNF mat loadings for the storage modulus and 0.98, 2.06% ECNF mat loadings for Young's modulus, even though the glass transition temperature (T_g), values dropped at all these extents of ECNF mat contents when compared with the neat epoxy resin.

Keywords: Carbon nanofibers; Dynamic mechanical analysis; Electrospun nanofibers; Epoxy nanocomposites; Flexural strength; Nanofiber mats; Tensile strength

Received 14 July 2008; in final form 23 January 2009.
Presented in part at the 2nd International Conference on Advanced Computational Engineering and Experimenting (ACE-X 2008), Barcelona, Spain, 14–15 July, 2008.
Address correspondence to Erol Sancaktar, Polymer Engineering Department, University of Akron, Akron, OH 44325-0301, USA. E-mail: erol@uakron.edu

1. INTRODUCTION

The advantages of conducting materials in the non-woven nanofiber-mat form prepared by the electrospinning technique are ideal for sensing nanocomposite applications. Due to the sub-micron size of electrospun conducting fibers, a large specific surface area is generated, while the fiber web contains high fiber aspect ratio and high interconnecting network compared with the same materials in film and short fiber forms. Consequently, electrospun polyacrylonitrile (PAN) fiber precursor based carbon (ECNF) nanofiber-based mats were produced and impregnated with epoxy resin. The mechanical properties of as-prepared nanofibers in the mat and short fiber filled epoxy nanocomposite forms were determined to demonstrate the effect of fiber aspect ratio and interconnecting network on those properties.

It is well known that metallic materials are excellent conducting fillers commonly used for improving the electrical properties of polymer composites, when included above their percolation threshold. A large portion of such applications include electrically conductive adhesives [1–6].

Metal-coated non-conductive or low-conduction fillers can also be used to induce electrical conductivity in polymer composites. Dilsiz *et al*. [7] coated spindle-type hematite and magnetite particles and nickel filaments with silver by using chemical reduction. The concentration of the reactants, the reaction time, and the type of reducing agent greatly influenced the morphology of the silver coating and the conductivity of the coated particles.

Due to the sub-micron size of electrospun conducting fibers, a large specific surface area is generated, with the fiber web containing high fiber aspect ratio and high interconnecting network compared with other conducting fillers used in comparable volume fractions. These characteristics are expected to enhance the electrical conduction [3,4], as well as the mechanical properties [5,8–11] of polymer-matrix nanocomposites to be manufactured using these nanofibers.

Mechanical properties of electrospun nanofibers, including tensile strength and Young's modulus, are mainly affected by their nanostructured surface with small pores. Gibson *et al*. [12] showed that the Young's modulus of electrospun pellethane thermoplastic elastomers was quite unchanged. On the other hand, a 40% reduction in tensile strength and 60% reduction in elongation were observed at maximum applied stress for pellethane electrospun elastomers compared with their cast film. Buchko *et al*. [13] reported a reduction of tensile strength for silk-like polymer with fibronectin functionality (SLPF)

fibers. For nanofiber-reinforced styrene-butadiene rubber, it was reported [14] that the Young's modulus of the nanofiber composite was ten-fold greater than the pure material at 10 phr nanofiber content. On the other hand, information on the mechanical properties of nanofibers and nanofiber composites has, so far, been very limited.

It has been reported that nanotubes increase the composite strength by as much as 25% [15]. However, multiwall nanotubes (MWNTs) are limited in their applications because of weak inter-shell interaction [16]. Single wall nanotubes (SWCNTs), on the other hand, are quite expensive and difficult to manufacture. Alternative reinforcement materials for nanocomposites include graphitic carbon nanofibers (GCNFs) and graphite nanoplatelets. GCNFs also have excellent properties and can be used as reinforcements in various kinds of matrices. They offer chemically facile sites that can be functionalized with additives, thereby resulting in a strong interfacial bond with the matrix.

Generally, the three main mechanisms of interfacial load transfer are micromechanical interlocking, chemical bonding, and the weak van der Waals forces between the matrix and the reinforcement [17]. From the length-scale argument it is known that the effective toughening may not be energetically favorable at the nano length-scale [18]. This generally necessitates a filler size greater than 100 nm [19]. There might be significant differences in mechanical behaviors between a continuous fiber-reinforced composite (*e.g.*, carbon fiber-reinforced composites, reinforced concrete) and a nanofiber-reinforced composite, even if both have very strong interfacial bonding. It has been proven that a continuous fiber-reinforced composite can effectively arrest the propagation of a major crack (which determines the material strength and toughness), while short nanofiber/nanotubes may lack this advantage [20].

To achieve maximum utilization of the properties of nanofibers, uniform dispersion and good wetting of the nanofibers within the matrix must be ensured. It has been extensively reported that dry nanofibers often agglomerate, and thereby greatly reduce their ability to bond with the matrix. All these local interfacial properties will affect the macro-level material behavior. For example, it was reported that there was as much as a 10% decrease in flexural strength in nanotube-epoxy composite beams due to weakly bonded interfaces [21]. Low-power ultrasonication is helpful in dispersing nanofibers and improving mechanical properties while high-power sonication may damage the molecular structures. The flexure failure of nanocomposite specimens was determined to be rather brittle compared with pure epoxy specimens [22]. Similar experiments showed that while there was a slight increase in stiffness and strength of nanofiber/PEEK composites,

there was a continuous decrease of the failure strain with increasing concentrations of nanofibers [23].

In this work, the mechanical properties of as-prepared nanofibers in the mat and short fiber-filled epoxy nanocomposite forms was characterized to demonstrate the effect of fiber aspect ratio and interconnecting network on those properties. The characterization of samples was performed by using scanning electron microscope (SEM), dynamic mechanical analyzer (DMA), and tensile testing.

2. EXPERIMENTAL METHODS AND MATERIALS

In this study, the electrospinning method was used to make carbon nanofibers (CNFs).

2.1. CNFs Via Electrospinning (ECNFs)

The spinning solutions were obtained from 6.5 PAN (Molecular Weight, M.W. = 150,000 from Scientific Polymer Products, Inc., Ontario, New York) dissolved in dimethylformamide (DMF) purchased from EMD Chemicals, Inc., (Gibbstown, NJ, USA) and then stirred at 60°C for 1 h [24–28] to get light yellow clear solutions. The as-prepared PAN solutions were subsequently electrospun under 20 kV applied voltage with 30 cm gap distance between the tip of the pipette and the collector (Fig. 1). The diameter of the pipette tip section was

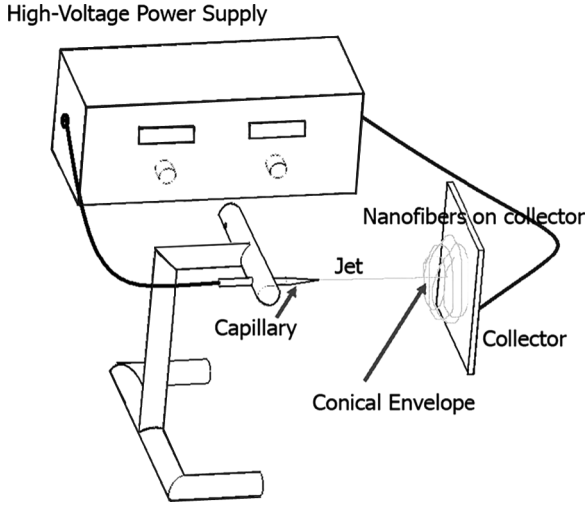

FIGURE 1 Schematic of the electrospinning setup.

roughly 0.1 mm. The electrospun PAN nanofiber mat was dried in the vacuum oven overnight at 60°C before heat stabilization in air at 280°C for 1 h and carbonization under N_2 flow at 950°C for 1 h in order to obtain the CNF mat [26–28]. SEM images of ECNF mat and short ECNF obtained by manually chopping the ECNF mat in a mortar are shown in Fig. 2.

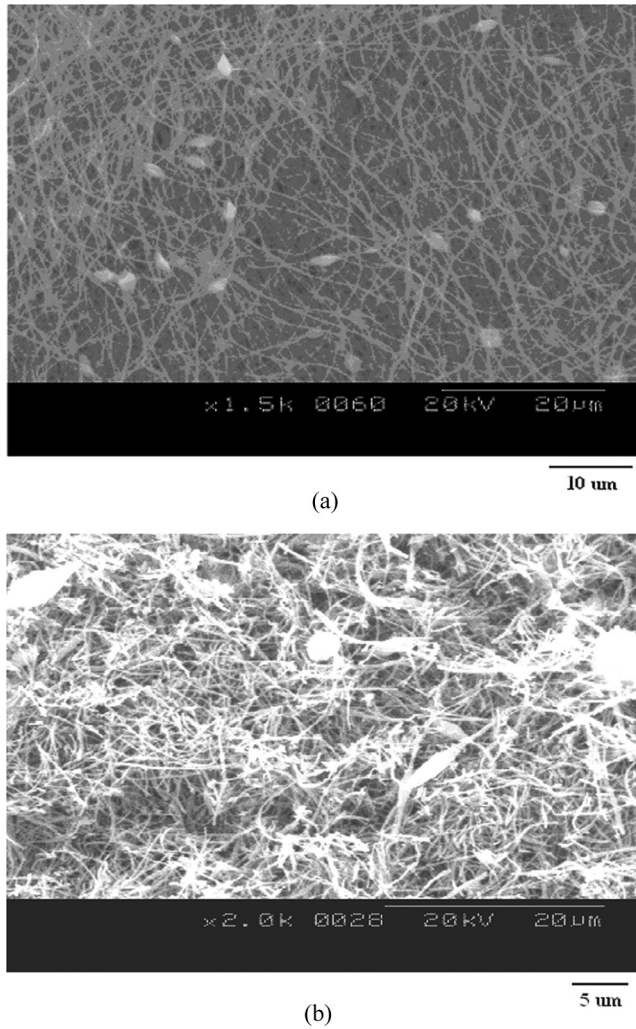

FIGURE 2 (a) Electrospun carbon nanofiber (ECNF) mat and (b) short ECNF obtained by manually chopping the ECNF mat in a mortar.

2.2. Preparation of Epoxy Nanocomposites

Composite specimens were prepared from plies of non-woven ECNF fabrics obtained as described above and impregnated with epoxy resin. 89.0 wt% epoxy resin (Epon815C, Shell Chemicals, Houston, TX, USA) and 11.0 wt.% diethylenetriamine (DETA, Epikure 3223, Resolution Performance Products, Houston, TX, USA), were mechanically mixed by using a magnetic bar for 10 min prior to impregnation. The cure reaction was done at 150°C for 30 min under compression molding at 2000 psi (13.8 Mpa). The sample was allowed to cool slowly to room temperature.

Specimens, 40.0 mm long, 6.5 mm wide, and 0.7 mm thick, were cut from the molded sheets of epoxy nanocomposites filled with ECNFs both in the mat and short nanofiber forms for the dynamic mechanical analysis (DMA) tests. In addition, specimens were also cut from the ECNF mat-epoxy and short ECNF-epoxy composite sheets into a rectangular shape with a cross section of about 0.4×4.0 mm and a gage length of around 20 mm for tensile, and $0.4 \times 4.0 \times 30.0\,mm^3$ for flexural tests, respectively. Two kinds of the specimens were prepared,

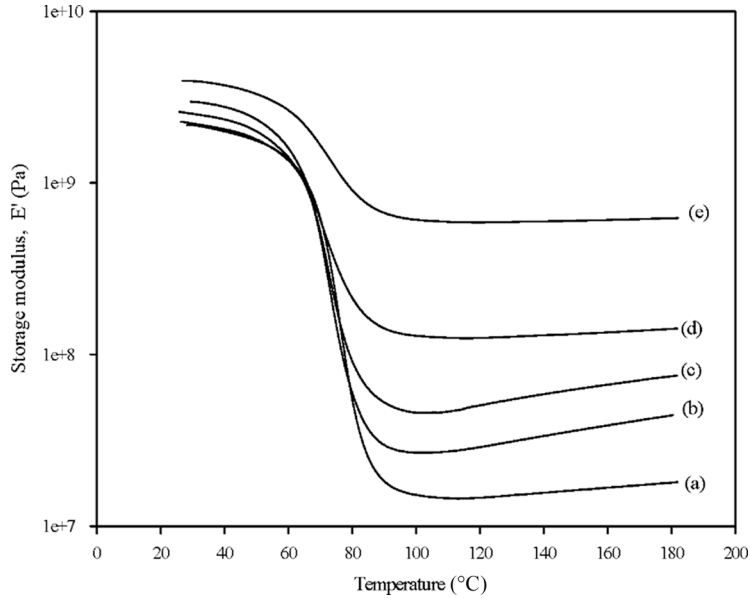

FIGURE 3 Storage moduli (E′) of epoxy nanocomposites as a function of temperature at 1.0 Hz for (a) cured epoxy resin, and its composites with ECNF mats (6.5 wt.% PAN solution): (b) 0.66 wt.%, (c) 1.23 wt.%, (d) 3.56 wt.%, and (e) 9.28 wt.%.

the bulk matrix without reinforcement and the non-woven ECNF mat filled epoxy nanocomposite.

In the case of short nanofiber-epoxy nanocomposites, each of the as-prepared conductive nanofiber materials was manually ground using a mortar and then sonicated (Sonicating bath, Branson 2510, American Laboratory Trading LLC, Groton, CT, USA) with 89 wt.% epoxy resin (Epon815C) for 1 h at room temperature before manually mixing with 11 wt.% DETA (Epikure 3223) for 10 min. The initial suspension before sonication showed a dark ring made up of the short nanofibers, in a white suspension made of the epoxy resin, indicating poor dispersion. After sonication, the improvement of dispersion was observed as a homogeneous black solution.

2.3. Mechanical Testing

2.3.1. Dynamic Mechanical Analyzer (DMA)

For DMA characterization, the complex modulus is written as:

$$E^* = E' + iE'', \tag{1}$$

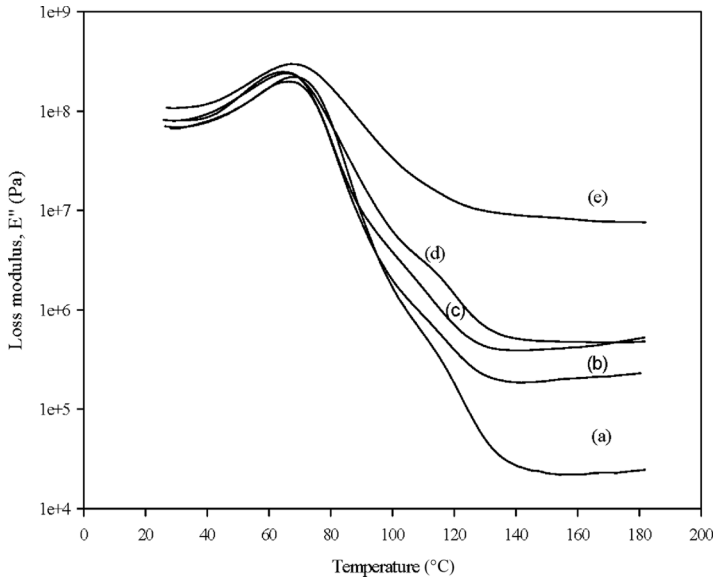

FIGURE 4 Loss moduli (E″) of epoxy nanocomposites as a function of temperature at 1.0 Hz for (a) cured epoxy resin, and its composites with ECNF mats (6.5 wt.% PAN solution): (b) 0.66 wt.%, (c) 1.23 wt.%, (d) 3.56 wt.%, and (e) 9.28 wt.%.

where E^* is the complex modulus, E' is the storage modulus, and E'' is the loss modulus. The ratio between E' and E'', the so, called tan delta ($\tan\delta$), or loss factor (damping), shows the loss of energy in the heat form resulting from the viscoelastic properties of polymers. Since the polymer has viscoelastic properties containing both elastic and viscous components, the complex modulus is the vectorial sum of the moduli representing those two components.

A DMA (Pyris Diamond DMA, Perkin Elmer, Inc., Fremont, CA, USA) was used to determine the storage modulus (E', G'), loss modulus (E'', G'') and $\tan\delta$ of epoxy nanocomposites, containing different non-woven ECNF mat and short ECNF loadings. The temperature was varied from 25 to 250°C using the tensile oscillating mode at 1 Hz and a gap length of 2 cm. Glass transition temperature (T_g) was defined as the $\tan\delta$ peak temperature.

2.3.2. Tensile Test

The mechanical behaviors of ECNFs-based epoxy composites were investigated for both fiber mat and short fiber forms by tensile tests,

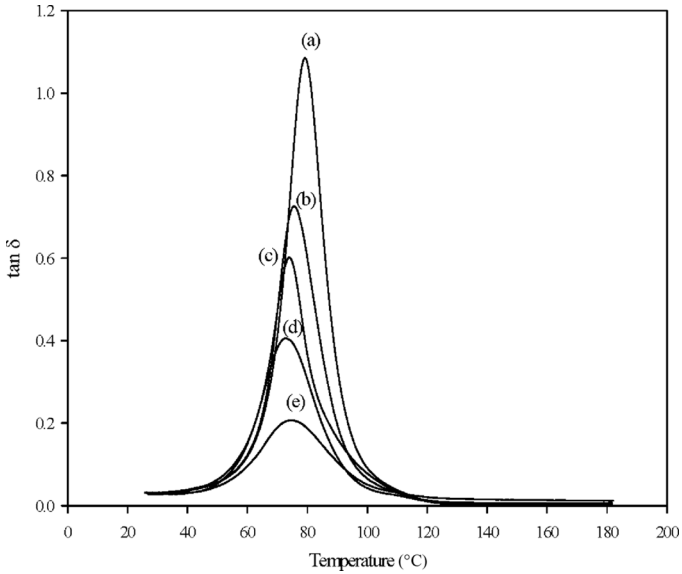

FIGURE 5 Loss factor ($\tan\delta$) of epoxy nanocomposites as a function of temperature at 1.0 Hz for (a) cured epoxy resin, and its composites with ECNF mats (6.5 wt.% PAN solution): (b) 0.66 wt.%, (c) 1.23 wt.%, (d) 3.56 wt.%, and (e) 9.28 wt.%.

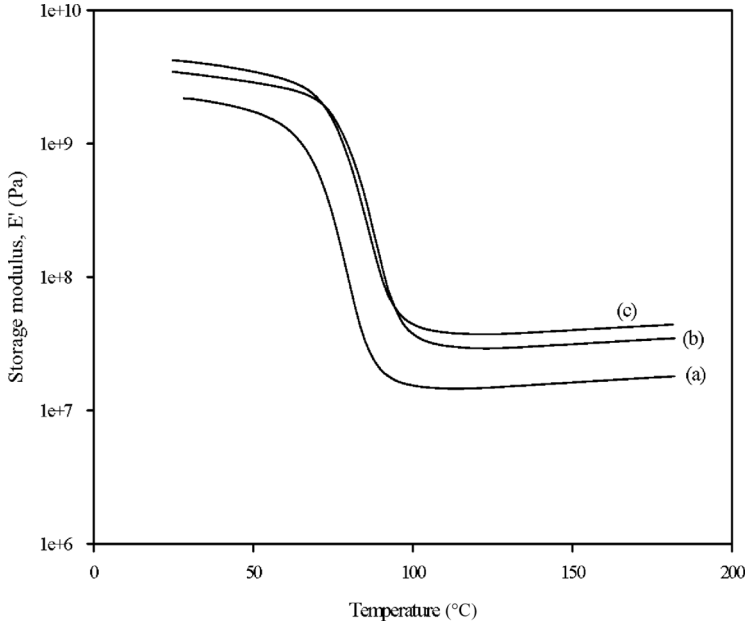

FIGURE 6 Storage moduli (E′) of epoxy nanocomposites as a function of temperature at 1.0 Hz for (a) cured epoxy resin, and its composites with short ECNFs (6.5 wt.% PAN solution): (b) 1.23 wt.% and (c) 2.06 wt.%.

in order to evaluate the effect of filler loading in the polymer domain. Tensile tests were performed at room temperature, approximately 25°C, on an Instron (Norwood, MA, USA) 5567 machine using a 1 kN load cell and a crosshead speed of 5 mm/min. Strain magnitudes were calculated by dividing the deformational extension values measured by the tensile tester with the specimen's gage length (20 mm). The $0.4 \times 4.0 \times 20$ mm specimens cut from the ECNF mat-epoxy and short ECNF-epoxy composites and neat epoxy sheets, into a rectangular shape, were hand-sanded by 300 grit sandpaper to remove flash and other edge effects and, subsequently, to carefully reduce the sample widths to 2.0 mm. At least three specimens were tested for each epoxy nanocomposite, containing different ECNF loadings. Small deviations were observed in mechanical performances.

2.3.3. Flexural Test

Tensile stresses were created at the outer surface of the film samples by flexing the film sample around various diameter cylinders. The maximum flexural tensile stress at break was determined by

using the following equation [29]:

$$\sigma_{max} = E[(h/2)/r], \quad (2)$$

where σ_{max} is the maximum flexural tensile stress at break (MPa), E is Young's modulus (MPa), h is the thickness of the specimen (mm) ≈ 0.4 mm, and r is rupture radius.

3. RESULTS AND DISCUSSION

3.1. Dynamic Mechanical Analysis (DMA)

The storage modulus (E′) and loss modulus (E″) *versus* temperature plots for various ECNF mat loadings in the epoxy nanocomposites are shown in Figs. 3 and 4, respectively, along with the corresponding tan δ plots in Fig. 5. The epoxy matrix displays typical behavior of amorphous thermoset polymers. At low temperature, the epoxy resin is in the glassy state and the storage modulus decreases slightly with increasing temperature, but remains around 1.5 GPa. Slight increases in E′ were observed in the glassy state with increasing

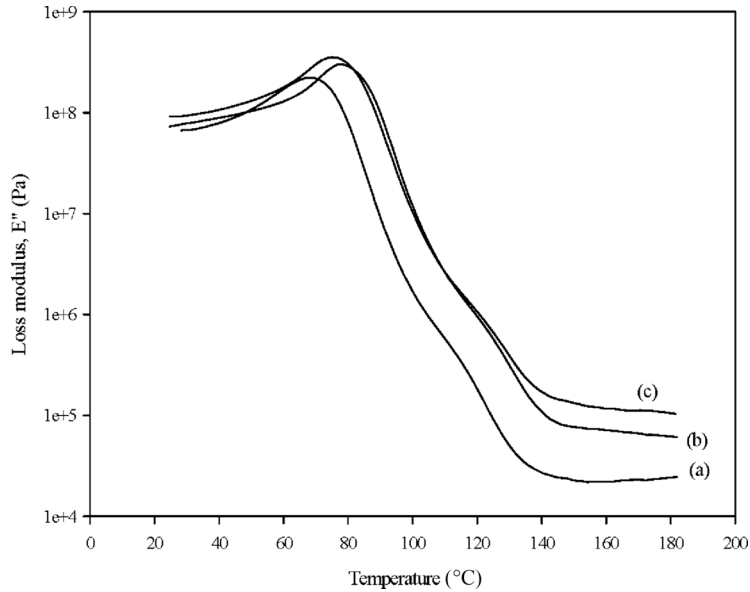

FIGURE 7 Loss moduli (E″) of epoxy nanocomposites as a function of temperature at 1.0 Hz for (a) cured epoxy resin, and its composites with short ECNFs (6.5 wt.% PAN solution): (b) 1.23 wt.% and (c) 2.06 wt.%.

ECNF mat content above 1.23 wt.% due to the large difference in moduli between the fibers and the matrix, and the high aspect ratio of the ECNF mat. Around 75°C, a rapid decrease in the elastic part of the modulus is observed while tan δ passes through a maximum. This relaxation phenomenon is associated with energy dissipation involving cooperative motions of long chain sequences, in relation with the glass transition phenomenon. Then, the elastic part of the modulus, E′, value reaches a plateau (rubbery modulus) approximately at 20 MPa. As seen in Fig. 3, the increase of modulus with increasing ECNF mat content is higher in the rubbery plateau than in the glassy state because of the larger contrast of moduli between the fibers and the matrix.

In the glassy state, the loss moduli increase slightly with increasing temperature, and a slight increase is observed in E″ with increasing ECNF mat content above 1.23 wt.% (Fig. 4). As observed with E′, the increase of modulus with increasing ECNF mat content is much higher for E″ in the rubbery plateau than in the glassy state.

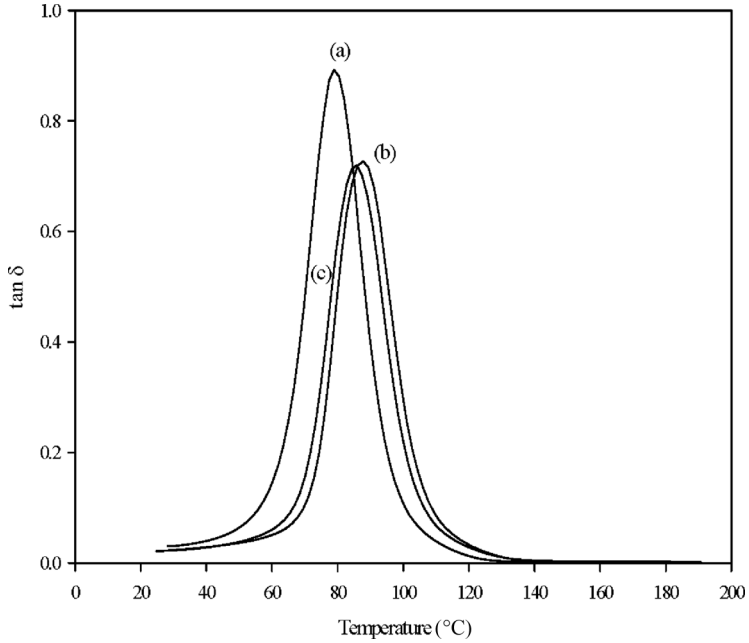

FIGURE 8 Loss factor (tan δ) of epoxy nanocomposites as a function of temperature at 1.0 Hz for (a) cured epoxy resin, and its composites with short ECNFs (6.5 wt.% PAN solution): (b) 1.23 wt.% and (c) 2.06 wt.%.

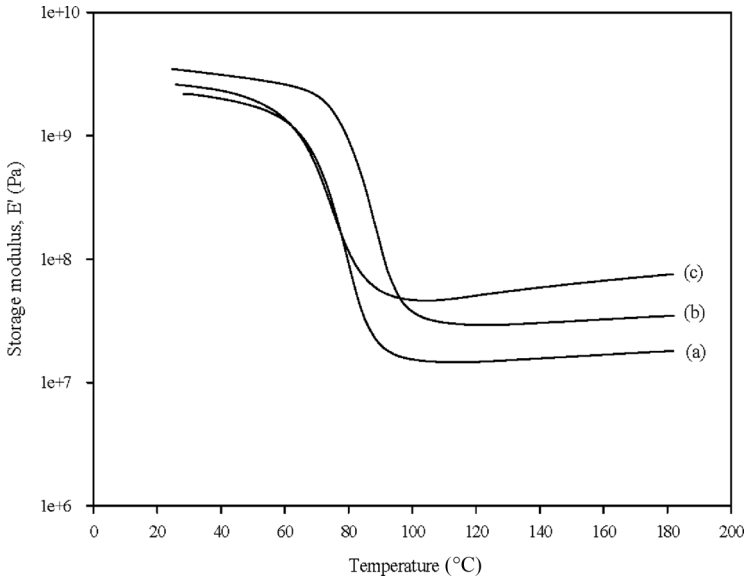

FIGURE 9 Storage moduli (E′) of epoxy nanocomposites as a function of temperature at 1.0 Hz for (a) cured epoxy resin, and its composites: (b) 1.23 wt.% short ECNFs (6.5 wt.% PAN solution) and (c) 1.23 wt.% ECNF mats (6.5 wt.% PAN solution).

It can be observed from Fig. 5 that the main mechanical relaxation of the epoxy matrix is modified by the presence of ECNF mats. The temperature of the maximum tan δ peak is firstly changed to lower temperatures at low fiber loadings (0.66, 1.23, and 3.56 wt.% loadings) and then increased slightly at the higher fiber loading of 9.28 wt.%. We note that this increase in the peak tan δ temperature at 9.28 wt.% fiber loading, however, did not bring this temperature level above that for the cured neat resin. The magnitude of the tan δ peak decreased as the amount of ECNF mat increased. The T_g of pure epoxy in this study was observed at approximately 80°C. It is well known that the T_g in filled polymers is dependent on the filler loading. The initial drop in T_g may be related to adsorption/deactivation of the curing agent by CNF mats, which lower crosslinking densities as the fiber loading goes up [30]. Xu *et al*. showed that vapor grown carbon fibers (VGCF) adsorb and/or deactivate the catalyst system, resulting in the drop in T_g of VGCF-vinyl ester composites. At a certain extent of ECNF mat, the T_g of the epoxy nanocomposite began to increase due to the effect of ultra-strength ECNF mats, which overcame the adsorption/deactivation effect. The E′ and E″ values increased markedly with

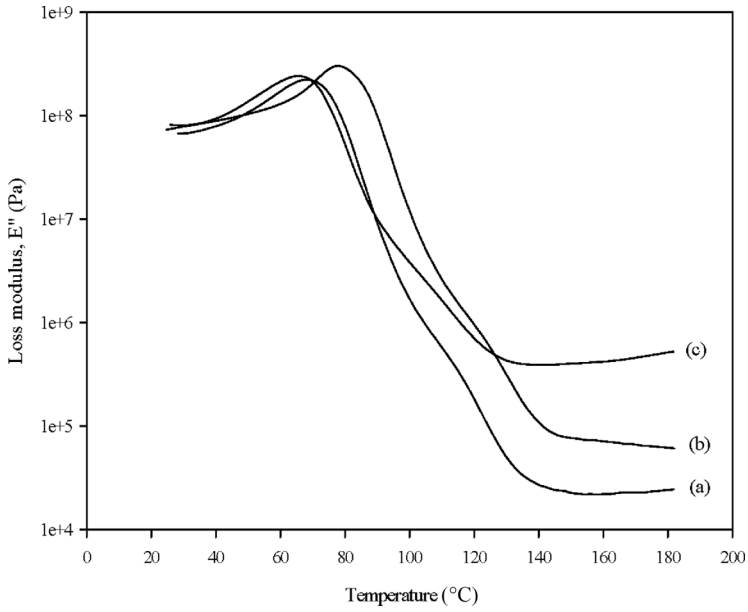

FIGURE 10 Loss moduli (E″) of epoxy nanocomposites as a function of temperature at 1.0 Hz for (a) cured epoxy resin, and its composites: (b) 1.23 wt.% short ECNFs (6.5 wt.% PAN solution) and (c) 1.23 wt.% ECNF mats (6.5 wt.% PAN solution).

fiber loading, reflecting the ability of the high aspect ratio fibers to stiffen the overall composite material.

The storage (E′) and loss moduli (E″) *versus* temperature plots for different short ECNF contents in the epoxy nanocomposites are shown in Figs. 6 and 7, respectively, together with the corresponding tan δ plots in Fig. 8. E′ and E″ both increased in the glassy state and in the rubbery plateau with increasing short ECNF contents of 1.23 and 2.06 wt.%. The variations of E′ and E″ with temperature and short fiber content (Figs. 6 and 7, respectively) were similar to those observed with long (ECNF) fibers (Figs. 3 and 4, respectively), except that, in the rubbery plateau region, increases in E′ and E″ values with short fiber loadings did not seem to be as pronounced as those with long fiber loadings. The temperature of the maximum tanδ peak shifted to a higher temperature at low fiber loading (1.23 wt.%) and then dropped slightly to lower temperature, while remaining above that for the cured neat resin, at higher fiber loading of about 2.06 wt.%. The magnitude of tan δ peak decreased as the amount of short ECNFs increased. By a differential scanning calorimetry (DSC) study, it has been reported that VGCFs did not affect

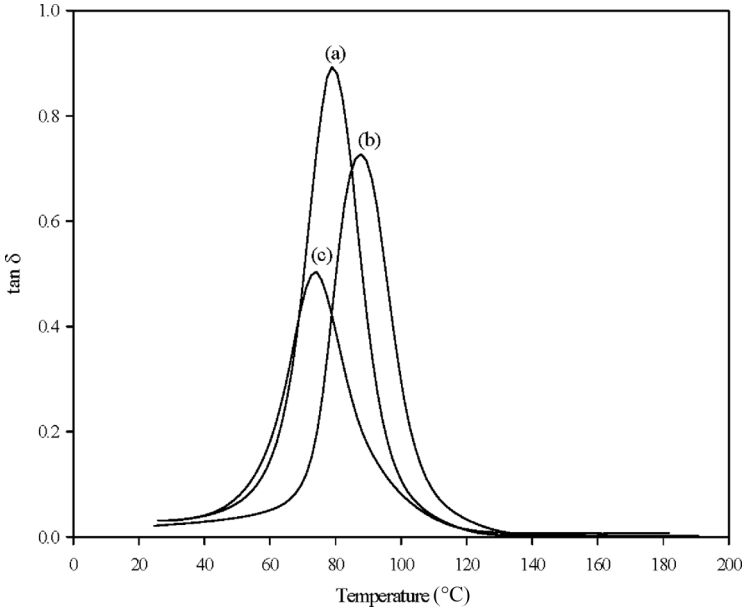

FIGURE 11 Loss factor ($\tan\delta$) of epoxy nanocomposites as a function of temperature at 1.0 Hz for (a) cured epoxy resin, and its composites: (b) 1.23 wt.% short ECNFs (6.5 wt.% PAN solution) and (c) 1.23 wt.% ECNF mats (6.5 wt.% PAN solution).

the cure reaction of an epoxy system at low filler contents [31]. However, the slight drop in T_g at 2.06 wt.% may be related to adsorption/deactivation of the curing agent by short ECNFs, which lowers crosslinking densities.

Both the E′ and E″ values at the rubbery state are lower for the nanocomposite with short ECNFs in comparison with that with ECNF mat-epoxy at 1.23 wt.% filler loading (Figs. 9 and 10, respectively), even though the T_g value for the nanocomposite with the ECNF mat is lower in comparison with that with short ECNFs at the same filler loading (Fig. 11). This reflects the ability of the high aspect ratio fibers to stiffen the overall composite material.

3.2. Tensile Properties

The true stress-strain curves [*i.e.*, $\sigma_{true} = \sigma(1+\varepsilon)$ and $\varepsilon_{true} = \mathrm{Ln}(1+\varepsilon)$, where σ and ε are engineering values] for both unfilled and filled epoxy resins are presented in Fig. 12. The observed behavior was a continuous increase of stress with strain until break. As the tensile

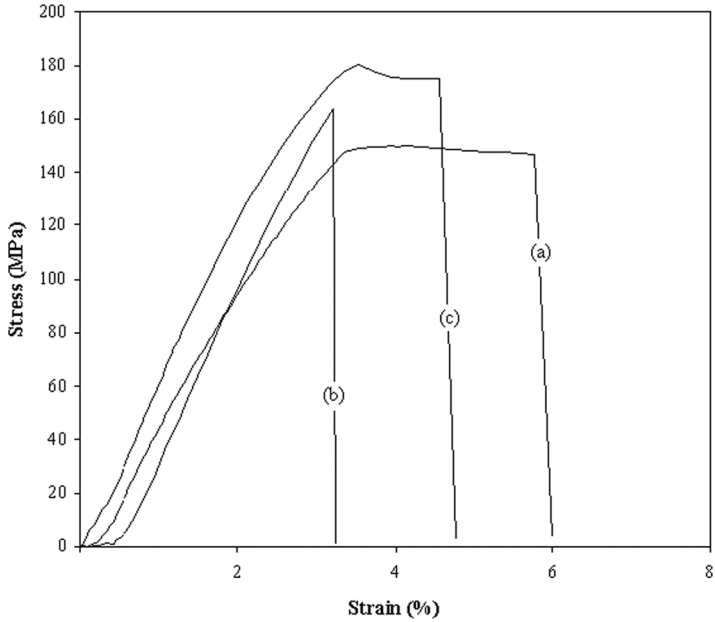

FIGURE 12 Tensile stress *versus* tensile strain for (a) cured epoxy resin, (b) 0.98 wt.% ECNF mat (6.5 wt.% PAN solution)-epoxy nanocomposite, (c) 2.06 wt.% ECNF mat (6.5 wt.% PAN solution)-epoxy nanocomposite.

test behavior is quasi-linear, the stress value, at a given strain level, increases with the amount of fibers along with the increasing of modulus. Epoxy nanocomposites containing ECNF mat exhibited larger stiffness, showing much lower tensile strain values, than neat epoxy resin. The toughness of these nanocomposites was not improved since the ultimate elongation of the matrix was drastically reduced at the expense of the increase in strength. The significant improvement of stiffness could be the consequence of strong filler-matrix interactions. The elastic moduli deduced from the stress–strain curves for the neat epoxy resin and its composites are shown in Fig. 13 as functions of ECNF mat and short fiber contents. These moduli values were calculated using the initial elastic portions of the stress-strain curves within 10% deviation. The ECNF mat-epoxy nanocomposites exhibited higher Young's moduli with increasing ECNF mat content, in comparison with neat epoxy resin. This result is in good agreement with the results from DMA measurements. The tensile modulus of the pure epoxy matrix was found to be 5.7 GPa and increased by 46% to 8.4 GPa when reinforced by 6.67 wt.% ECNF mat. The specific

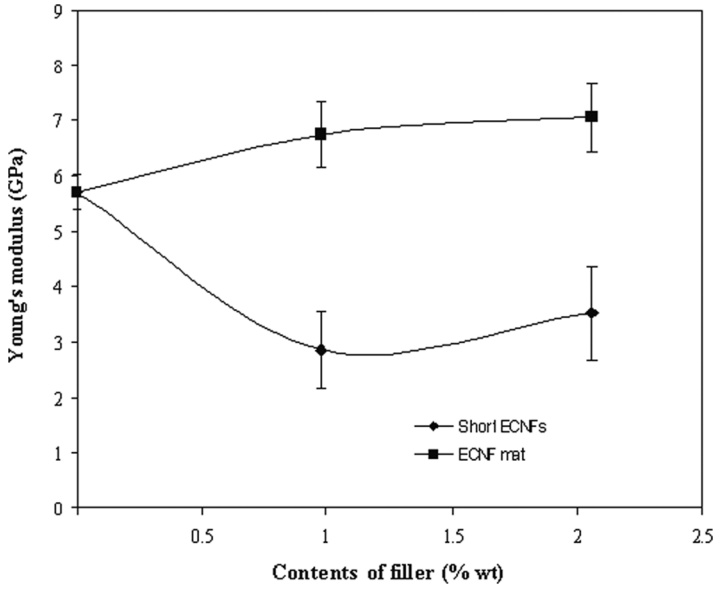

FIGURE 13 Young's moduli *versus* ECNF (6.5 wt.% PAN solution) contents in short nanofiber and mat forms for neat epoxy resin and its composites.

characteristics of ECNF mat in nanocomposites are: (a) large interfacial area and (2) reduction of average distance between the fibers. This can favor the short distance filler–filler interactions. Moreover, due to the large surface area, the polymer interphase layer, if it exists, is expected to play a dominant role in the properties of the nanocomposites. Thus, nano-sized filler with high aspect ratio provides the advantages of low percolation threshold and large interfacial area. The presence of adhesive bonding, which enables load transfer from the matrix to the ECNF mat, may be the key parameter influencing the increase in strength.

The effect of the high aspect ratio of ECNFs on tensile properties was also studied by comparing epoxy nanocomposites containing ECNF mat and short ECNFs as fillers. Figure 14 shows tensile stress *versus* strain curves for short ECNF-epoxy nanocomposites with 0.98 and 2.06 wt.% short ECNF contents. The characteristics of tensile curves for short ECNF-epoxy nanocomposites before break are different when compared with ECNF mat-epoxy nanocomposites. The linear relationship between stress and strain up close to break has deteriorated. The Young's moduli values of short ECNF-epoxy nanocomposites also dropped dramatically, when compared with neat epoxy

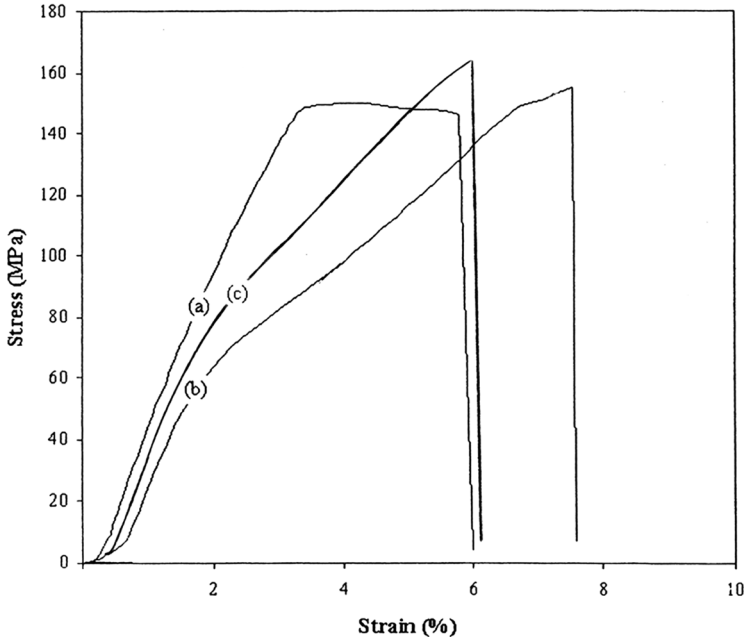

FIGURE 14 Tensile stress *versus* tensile strain for (a) cured epoxy resin, (b) 0.98 wt.% short ECNFs (6.5 wt.% PAN solution)-epoxy nanocomposite, and (c) 2.06 wt.% short ECNFs (6.5 wt.% PAN solution)-epoxy nanocomposite.

resin and ECNF mat-epoxy nanocomposites (Fig. 13). We note that such reductions in Young's moduli with the addition of short ECNFs to neat epoxy seems to contradict the increases in E′ values observed in the glassy state of the short ECNF-epoxy nanocomposite using DMA (Fig. 6). The authors believe that this discrepancy is due to the large difference in displacement levels used in DMA in comparison with the standard tensile testing procedure. The displacement amplitude used in our DMA test was 10^{-8} m, whereas the Young's modulus was evaluated within displacement levels up to 2.5×10^{-4} m during tensile testing (Fig. 14). Therefore, it is more likely that many short fiber ends would cause more extensive nano-size damage zones in the epoxy material at these higher displacement levels of the tensile test, where the Young's moduli were evaluated, and result in distinct reductions in the nanocomposite stiffnesses. The poor reinforcement efficiency of short ECNFs were also revealed by the existence of fiber pull-out in the composites, observed in SEM images of the fracture surfaces (Fig. 15). It is clear that ECNF mats were more efficient

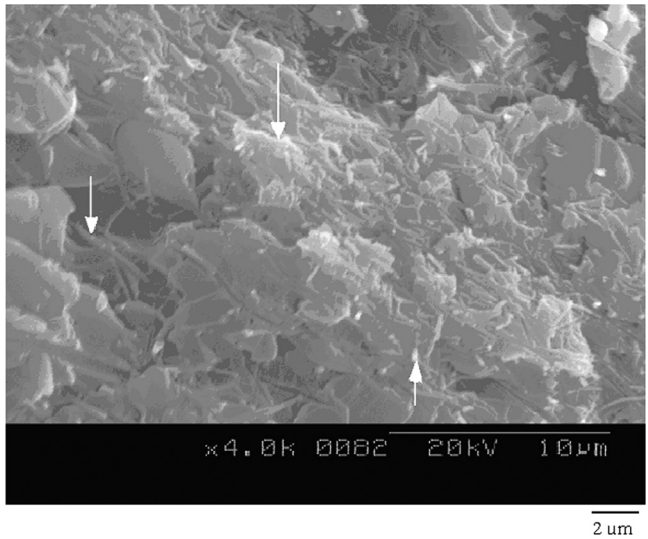

FIGURE 15 SEM images of a fracture surface for 2.06 wt.% short ECNF (6.5 wt.% PAN solution)-epoxy nanocomposite at high magnification (arrows locate pulled-out short ECNFs).

reinforcing fillers than short ECNFs, due to their higher aspect ratio. In this study, nanocomposites containing ECNF mats were easier to process and provided a higher degree of homogeneity compared to those containing short ECNFs.

3.3. Flexural Tensile Properties

The maximum flexural tensile stress (σ_{max}) value at the outer surfaces of neat epoxy samples was measured to be approximately 330 MPa as shown in Fig. 16. We note that this value is a little more than twice that of model epoxy tensile strength, which is approximately 150 MPa (Figs. 12 and 14). This finding reveals a superior resistance to flexural loading by our model epoxy material. When increasing amounts of the ECNF mat are added to this neat resin, however, the maximum flexural tensile stress at the outer surface decreased as a result of the embrittlement effect of the ECNF mat in the composites (Fig. 16). Note that this embrittlement effect, which reduced the flexural strength of the nanocomposite, was not observed with the tensile behavior, where the ultimate tensile strength increased with ECNF mat addition.

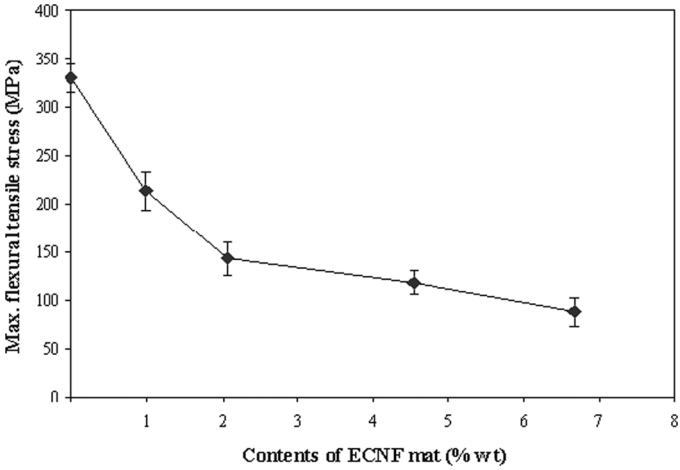

FIGURE 16 Maximum flexural tensile stress at the outer surface for neat epoxy resin and its composites at various ECNF mat (6.5 wt.% PAN solution) contents.

CONCLUSIONS

It was observed that epoxy nanocomposites containing ECNFs with high fiber aspect ratio in the non-woven mat form yield better mechanical properties than those filled with short ECNFs. The ECNF mat in epoxy nanocomposites provided better homogeneity and easier preparation than short ECNFs. Dynamic and monotonic tensile mechanical properties of ECNF mat-epoxy nanocomposites, such as E′ and E″, Young's modulus, and ultimate tensile strength all increased, while toughness and flexural strength decreased in comparison with the neat epoxy resin. The DMA results showed higher modulus for the ECNF mat-epoxy nanocomposites compared with the neat epoxy resin and short ECNF-epoxy nanocomposites. The ECNF-epoxy nanocomposites had higher storage and Young's moduli with 1.23, 3.56, and 9.28 wt.% ECNF mat loadings for the storage modulus and 0.98 and 2.06 wt.% ECNF mat loading for Young's modulus, even though the T_g values dropped at all these extents of ECNF mat contents compared with the neat epoxy resin.

REFERENCES

[1] Sancaktar, E. and Dilsiz, N., *J. Adhesion Sci. Technol.* **13**, 763–771 (1999).
[2] Sancaktar, E. and Dilsiz, N., *J. Adhesion Sci. Technol.* **13**, 679–693 (1999).
[3] Wei, Y. and Sancaktar, E., *J. Adhesion Sci. Technol.* **10**, 1199–1219 (1996).

[4] Sancaktar, E. and Wei, Y., *J. Adhesion Sci. Technol.* **10**, 1221–1235 (1996).
[5] Sancaktar, E., Wei, Y., and Gaynes, M. A., *J. Adhesion* **56**, 229–246 (1996).
[6] Sancaktar, E. and Dilsiz, N., *J. Adhesion Sci. Technol.* **11**, 155–166 (1997).
[7] Dilsiz, N., Partch, R., Matijevic', E., and Sancaktar, E., *J. Adhesion Sci. Technol.* **11**, 1105–1118 (1997).
[8] Sancaktar, E. and Zhang, P., *J. Mech. Design* **112**, 605–619 (1990).
[9] Sancaktar, E. and Beachtle, D., *J. Adhesion* **42**, 65–85 (1993).
[10] Sancaktar, E., *J. Adhesion Sci. Technol.* **9**, 119–147 (1995).
[11] Sancaktar, E., *Appl. Mech. Rev.* **49**, S128–S138 (1996).
[12] Gibson, H., Gibson, P., Senecal, K., Sennett, M., Walker, J., Yeomans, W., and Ziegler, D., *J. Adv. Mater.* **34**, 44–55 (2002).
[13] Buchko, C. J., Chen, L. C., Yu, S., and Martin, D. C., *Polymer* **40**, 7397–7407 (1999).
[14] Kim, J. S. and Reneker, D. H., *Polym. Comp.* **20**, 124–131 (1999).
[15] Qian, D., Dickey, E. C., Andrews, R., and Rantell, T., *Appl. Phys. Letts.* **76**, 2868–2870 (2000).
[16] Yu, M. F., Lourie, O., Dyer, M., Moloni, K., Kelly, T., and Ruoff, R. S., *Science* **287**, 637–640 (2000).
[17] Schadler, L. S., Giannaris, S. C., and Ajayan, P. M., *Appl. Phys. Letts.* **73**, 3842–3844 (1998).
[18] Zerda, A. S. and Lesser, A. J., *J. Polym. Sci. Part B: Polym. Phys.* **39**, 1137–1146 (2001).
[19] Bucknall, C. B., Karpodinis, A., and Zhang, X. C., *J. of Matls. Sci.* **29**, 3377–3383 (1994).
[20] Odegard, G. M., Gates, T. S., Wise, K. E., Park, C., and Siochi, E. J., *Comps. Sci. & Tech.* **63**, 1671–1687 (2003).
[21] Lau, K. T., Shi, S. Q., Zhou, L. M., and Cheng, H. M., *J. Comps. Matls.* **37**, 365–376 (2003).
[22] Xu, L. R., Bhamidipati, V., Zhong, W.-H., Li, J., Lukehart, C. M., Lara-Curzio, E., Liu, K. C., and Lance, M. J., *J. Comps. Mats.* **38**, 15631582 (2004).
[23] Sandler, J., Werner, P., Shaffer, M., Demchuk, V., Altstädt, V., and Windle, A., *Comp. A* **33**, 1033–1039 (2002).
[24] Kim, C. and Yang, K. S., *Appl. Phys. Lett.* **83**, 1216–1218 (2003).
[25] Wang, Y., Serrano, S., and Santiago-Avilés, J. J., *Synth. Met.* **138**, 423–427 (2003).
[26] Kim, C., Park, S.-H., Cho, J.-I., Lee, D.-Y., Park, T.-J., Lee, W.-J., and Yang, K.-S., *Raman Spect.* **35**, 928–933 (2004).
[27] Aussawasathien, D. and Sancaktar, E., *Current Nanoscience* **4**, 130–137 (2008).
[28] Aussawasathien, D. and Sancaktar, E., *Macromol. Symp.* **264**, 26–33 (2008).
[29] Riley, W. F., Sturges, L. D., and Morris, D. H., *Mechanics of Materials*, (John Wiley, New York, 1999), 5th ed., pp. 350–365.
[30] Xu, J., Donohoe, J. P., and, Pittman, C. U., Jr., *Comp. Part A: Appl. Sci. & Manuf.* **35**, 693–701 (2004).
[31] Xie, H. F., Liu, B. H., Yuan, Z. R., Shen, J. Y., and Cheng, R. S., *J. Polym. Sci. Part B: Polym. Phys.* **42**, 3701–3712 (2004).